

## Supplementary Information

**Table S1.** Conformer relative free energies with respect to the most stable form.

**Table S2.** Calculated binding energies ( $\Delta G$ ) for the most and least active compounds.

**Figure S1.** HR-ESI-FTMS spectrum of Sarcoehrenbergilid A (**1**).

**Figure S2.**  $^1\text{H}$  NMR spectrum of Sarcoehrenbergilid A (**1**) in  $\text{CDCl}_3$ .

**Figure S3.**  $^{13}\text{C}$  NMR spectrum of Sarcoehrenbergilid A (**1**) in  $\text{CDCl}_3$ .

**Figure S4.** DEPT spectrum of Sarcoehrenbergilid A (**1**) in  $\text{CDCl}_3$ .

**Figure S5.** HSQC spectrum of Sarcoehrenbergilid A (**1**) in  $\text{CDCl}_3$ .

**Figure S6.** HMBC spectrum of Sarcoehrenbergilid A (**1**) in  $\text{CDCl}_3$ .

**Figure S7.** NOESY spectrum of Sarcoehrenbergilid A (**1**) in  $\text{CDCl}_3$ .

**Figure S8.** HR-ESI-FTMS spectrum of Sarcoehrenbergilid B (**2**).

**Figure S9.**  $^1\text{H}$  NMR spectrum of Sarcoehrenbergilid B (**2**) in  $\text{CDCl}_3$ .

**Figure S10.**  $^{13}\text{C}$  NMR spectrum of Sarcoehrenbergilid B (**2**) in  $\text{CDCl}_3$ .

**Figure S11.**  $^1\text{H}$ - $^1\text{H}$  COSY spectrum of Sarcoehrenbergilid B (**2**) in  $\text{CDCl}_3$ .

**Figure S12.** HSQC spectrum of Sarcoehrenbergilid B (**2**) in  $\text{CDCl}_3$ .

**Figure S13.** HMBC spectrum of Sarcoehrenbergilid B (**2**) in  $\text{CDCl}_3$ .

**Figure S14.** NOESY spectrum of Sarcoehrenbergilid B (**2**) in  $\text{CDCl}_3$ .

**Figure S15.** HR-ESI-FTMS spectrum of Sarcoehrenbergilid C (**3**).

**Figure S16.**  $^1\text{H}$  NMR spectrum of Sarcoehrenbergilid C (**3**) in  $\text{CDCl}_3$ .

**Figure S17.**  $^{13}\text{C}$  NMR spectrum of Sarcoehrenbergilid C (**3**) in  $\text{CDCl}_3$ .

**Figure S18.** DEPT spectrum of Sarcoehrenbergilid C (**3**) in  $\text{CDCl}_3$ .

**Figure S19.** HSQC spectrum of Sarcoehrenbergilid C (**3**) in  $\text{CDCl}_3$ .

**Figure S20.** HMBC spectrum of Sarcoehrenbergilid C (**3**) in  $\text{CDCl}_3$ .

**Figure S21.** NOESY spectrum of Sarcoehrenbergilid C (**3**) in  $\text{CDCl}_3$ .

**Figure S22.** Optimized structure and relative free energy of conformers of **1** with Boltzmann population higher than 1%.

**Figure S23.** Optimized structure and relative free energy of conformers of **2** with Boltzmann population higher than 1%.

**Figure S24.** Optimized structure and relative free energy of conformers of **3** with Boltzmann population higher than 1%.

**Figure S25.** Anti-proliferative A549 response curves with **1-8** based on MTT-reduction assay.

**Figure S26.** Anti-proliferative Caco-2 response curves with **1-8** based on MTT-reduction assay.

**Figure S27.** Anti-proliferative HepG2 response curves with **1-8** based on MTT-reduction assay.

**Figure S28.** Calculated (i) Autodock and (ii) MM/GBSA binding energies of compounds with EGFR kinase domain relative to the experimental binding energies for the tested compounds against A549 cell line.

**Figure S29.** Hydrogen bond distance between **8** and carboxylate oxygen atom of Asp<sup>776</sup> inside EGFR active site.

**Table S1.** Conformer relative free energies with respect to the most stable form.

Compound	Conformer ID	Relative Free Energy $\Delta G$ (kJ/mol)	Boltzmann Factor <sup>a</sup> $e^{(-\Delta G/RT)}$	Population %	Optical Rotation (degree) <sup>b</sup>
1	1a	0.00	1.00	37.44	-244.3
	1b	+2.8	0.32	11.89	-204.1
	1c	+3.1	0.29	10.74	-16.5
	1d	+3.2	0.27	10.26	67.0
	1e	+4.2	0.18	6.75	33.2
	1f	+4.3	0.17	6.50	-127.6
	1g	+5.3	0.12	4.48	192.7
	1h	+7.0	0.06	2.18	88.2
	1i	+7.4	0.05	1.87	-85.7
2	2a	0.00	1.00	34.21	-88.5
	2b	+0.2	0.94	32.03	-89.5
	2c	+1.5	0.54	18.48	68.8
	2d	+4.4	0.17	5.82	223.6
	2e	+6.6	0.07	2.37	-37.8
	2f	+6.8	0.07	2.24	37.5
	2g	+7.4	0.05	1.70	38.4
					-32.6 <sup>c</sup>
3	3a	0.00	1.00	37.62	-162.84
	3b	+0.9	0.69	25.82	65.13
	3c	+4.0	0.20	7.41	-10.52
	3d	+5.5	0.11	4.11	-119.51
	3e	+5.9	0.09	3.47	-10.25
	3f	+6.0	0.09	3.34	-13.39
	3g	+6.0	0.09	3.33	132.21
	3h	+6.7	0.07	2.52	-96.37
	3i	+6.9	0.06	2.35	-40.38
	3j	+8.6	0.03	1.16	8.17
					-49.8 <sup>c</sup>

<sup>a</sup>Calculated at 298K.<sup>b</sup>Calculated at B3LYP/6-31G\* level of theory with the polarizable continuum model (PCM) for chloroform.<sup>c</sup>Boltzmann-weighted mean optical rotation.

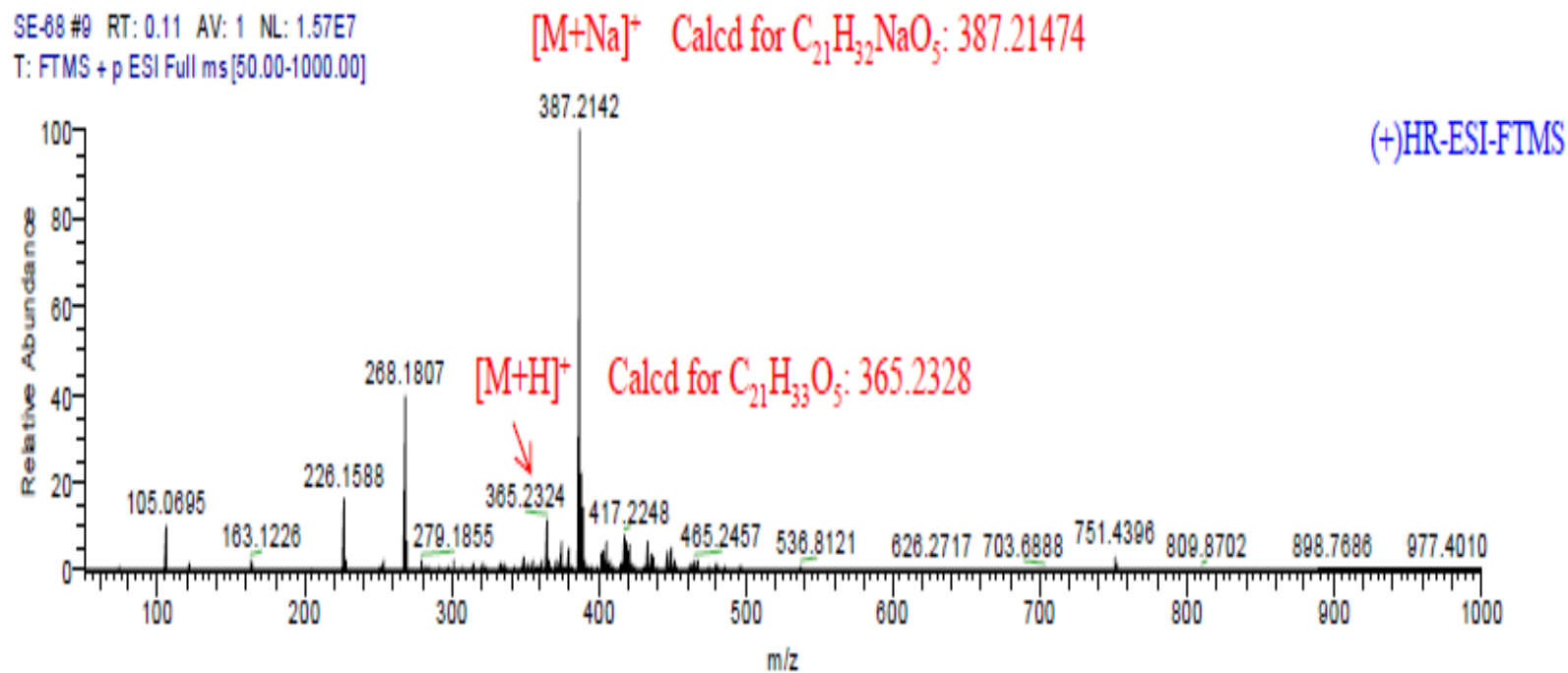
**Table S2.** Calculated auto-dock and MM/GBSA binding energies ( $\Delta G$ ) for the most and least active compounds complexed with the EGFR kinase domain.

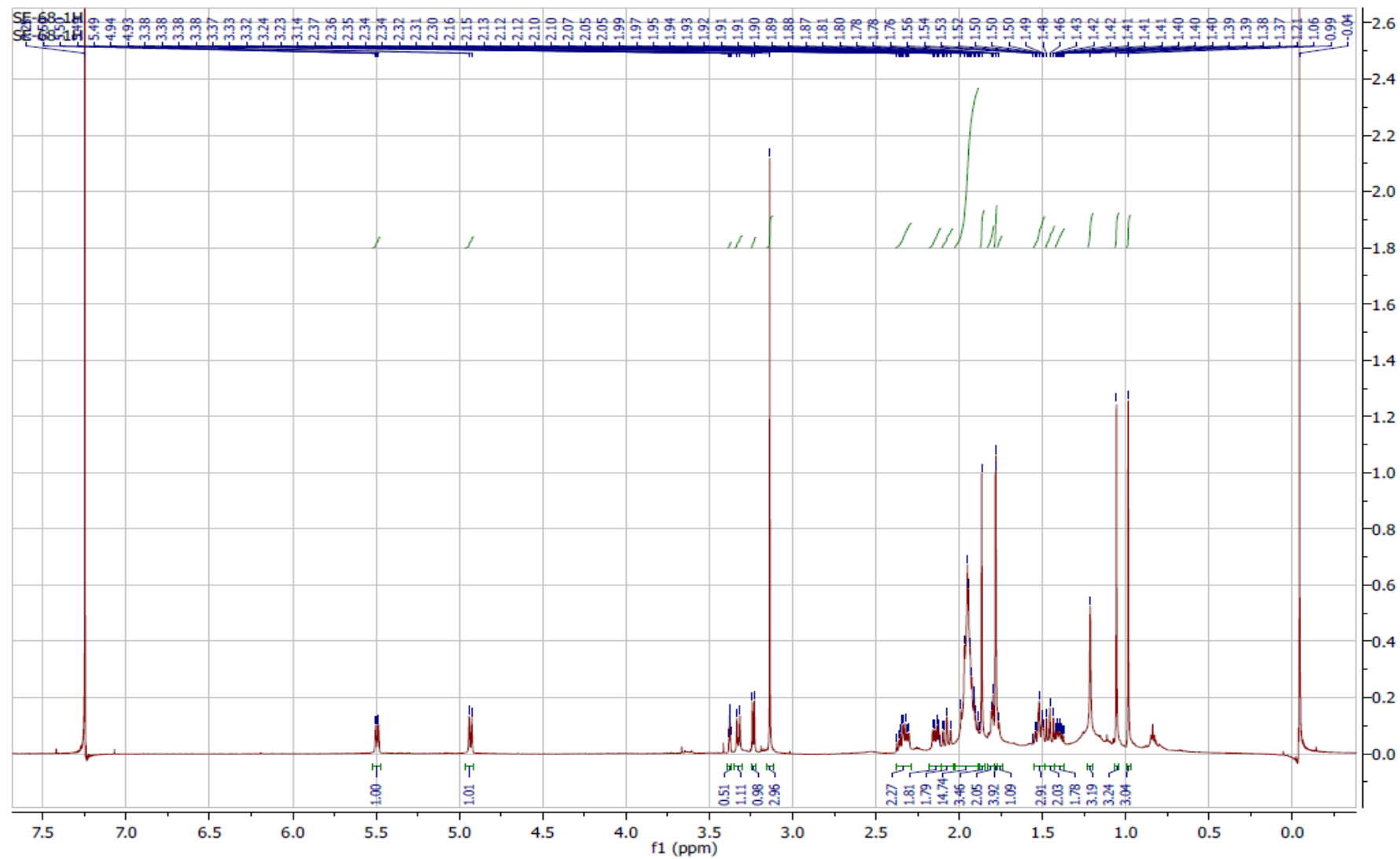
Compound	IC <sub>50</sub> ( $\mu$ M) <sup>a</sup>	$\Delta G_{\text{exp}}$ (kcal/mol) <sup>b</sup>	$\Delta G_{\text{calc}}$ (kcal/mol)		Binding Features		
			AutoDock	MM/GBSA	Residue	Type	Length ( $\text{\AA}$ )
Erlotinib	nd	---	-7.23	-47.89	Met <sub>769</sub>	H-bond	2.01
					Cys <sub>773</sub>	H-bond	2.05
Afatinib	nd	---	-7.68	-55.90	Met <sub>769</sub>	H-bond	2.09
					Leu <sub>694</sub>	H-bond	2.10
					Cys <sub>773</sub>	H-bond	1.90
					Lys <sub>692</sub>	H-bond	1.91
Gefitinib	nd	---	-7.69	-50.23	Thr <sub>766</sub>	H-bond	2.08
					Met <sub>769</sub>	H-bond	2.24
Doxorubicin	0.62	-8.46	-8.94	-54.72	Lys <sub>721</sub>	H-bond	1.92
					Thr <sub>766</sub>	H-bond	1.76
					Met <sub>769</sub>	H-bond	1.82
					Thr <sub>830</sub>	H-bond	1.92
					Asp <sub>831</sub>	H-bond	1.94
8	27.3	-6.22	-8.13	-41.18	Thr <sub>766</sub>	H-bond	1.79
					Asp <sub>776</sub>	H-bond	1.62
7	43.6	-5.94	-5.82	-36.52	Thr <sub>766</sub>	H-bond	1.75
					Thr <sub>830</sub>	H-bond	1.87
6	37.0	-6.04	-6.14	-38.04	Met <sub>769</sub>	H-bond	1.82
					Asp <sub>831</sub>	H-bond	1.65
4	91.5	-5.51	-7.17	-31.81	Lys <sub>721</sub>	H-bond	1.82
Correlation coefficient (R <sup>2</sup> )			0.37 <sup>c</sup>	0.96 <sup>c</sup>			

<sup>a</sup>IC<sub>50</sub> Values for the tested compounds against A549 cell line.

<sup>b</sup>Calculated based on the experimental IC<sub>50</sub>.

<sup>c</sup>Erlotinib, afatinib and gefitinib were not considered in the calculated correlation due to the absence of the corresponding experimental IC<sub>50</sub>.

**Figure S1.** HR-ESI-FTMS spectrum of Sarcoehrenbergilid A (1) in CDCl<sub>3</sub>.

**Figure S2.**  $^1\text{H}$  NMR spectrum of Sarcoehrenbergilid A (**1**) in  $\text{CDCl}_3$ .

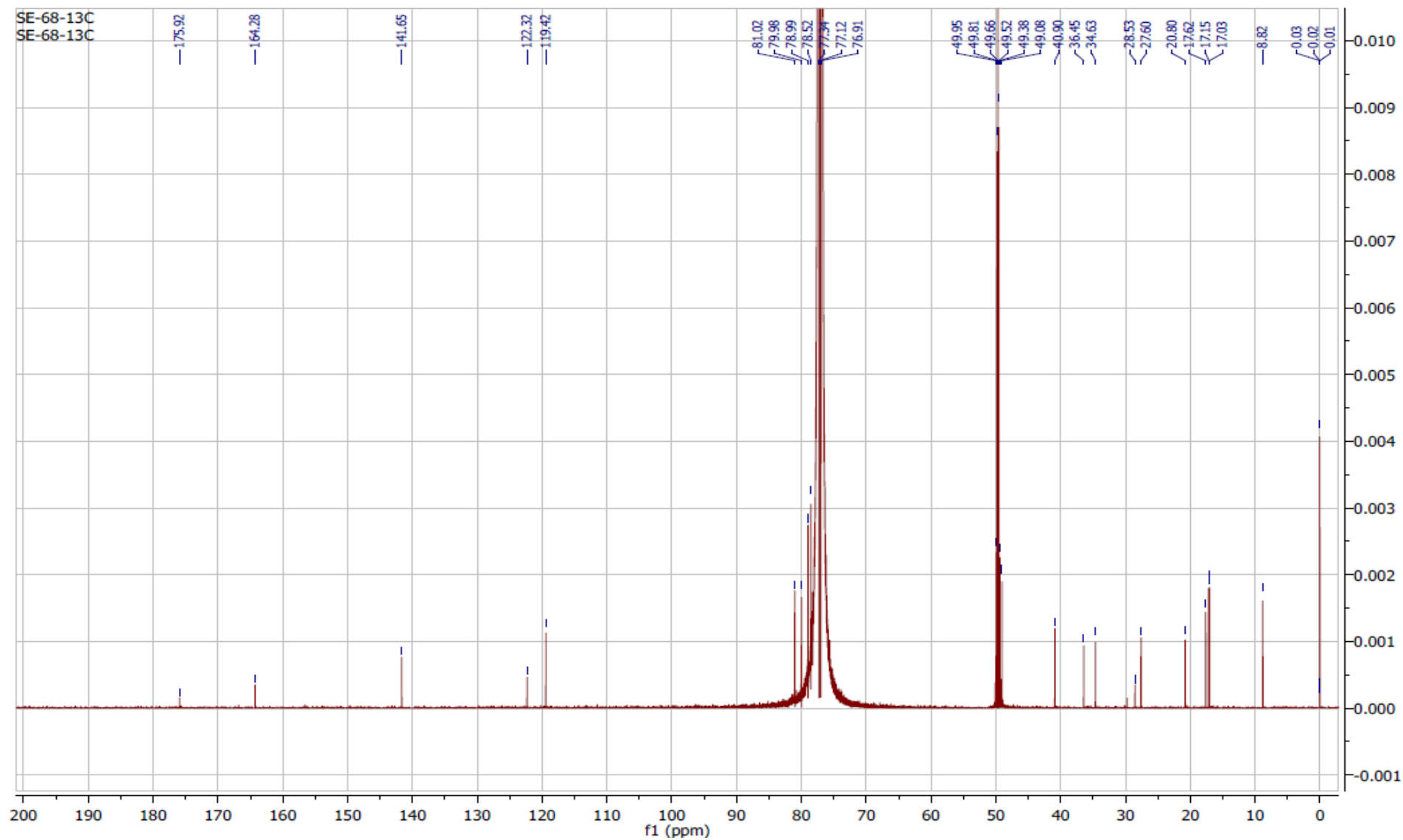
**Figure S3.**  $^{13}\text{C}$  NMR spectrum of Sarcoehrenbergilid A (**1**) in  $\text{CDCl}_3$ .

Figure S4. DEPT spectrum of Sarcoehrenbergilid A (1) in CDCl<sub>3</sub>.

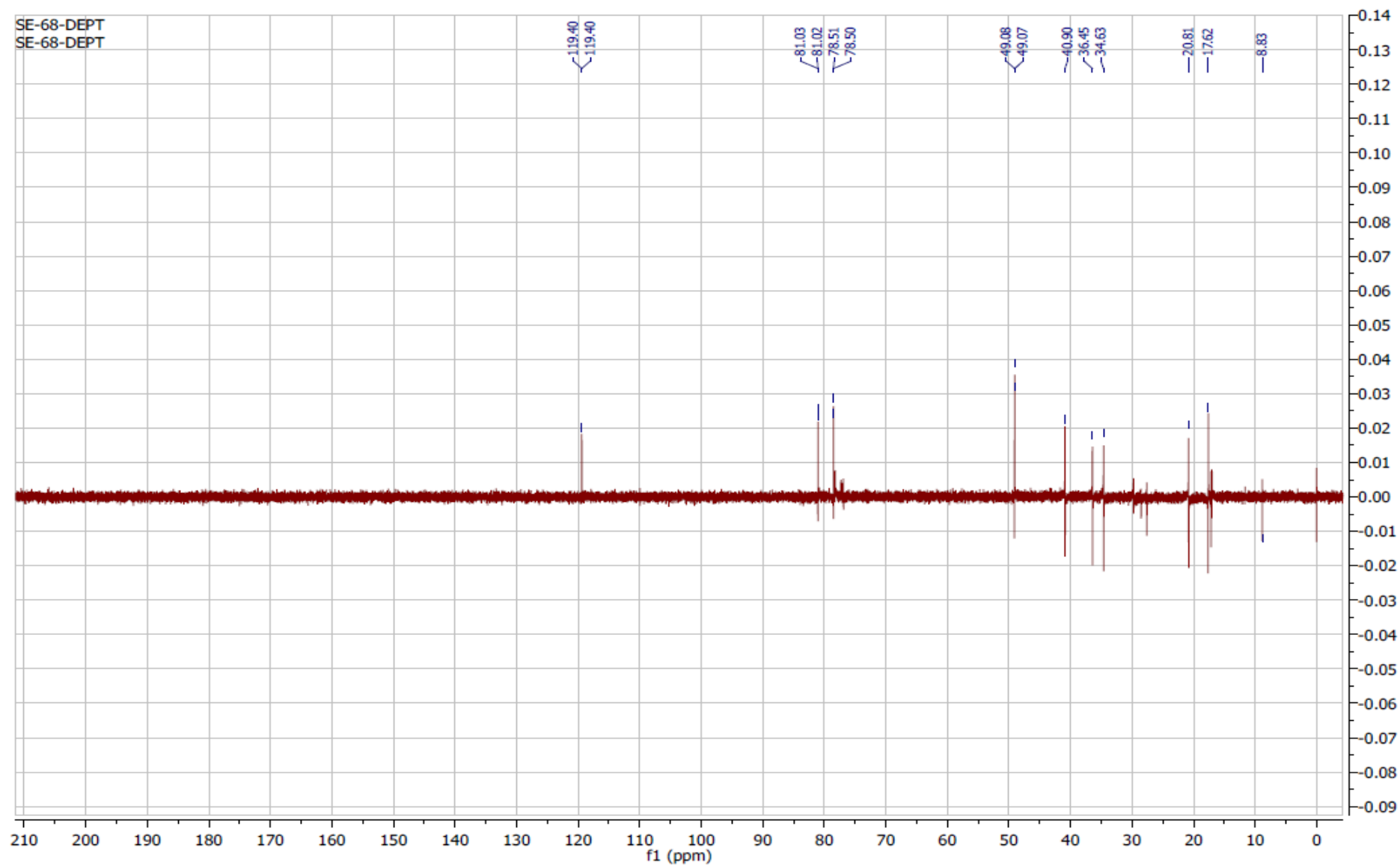
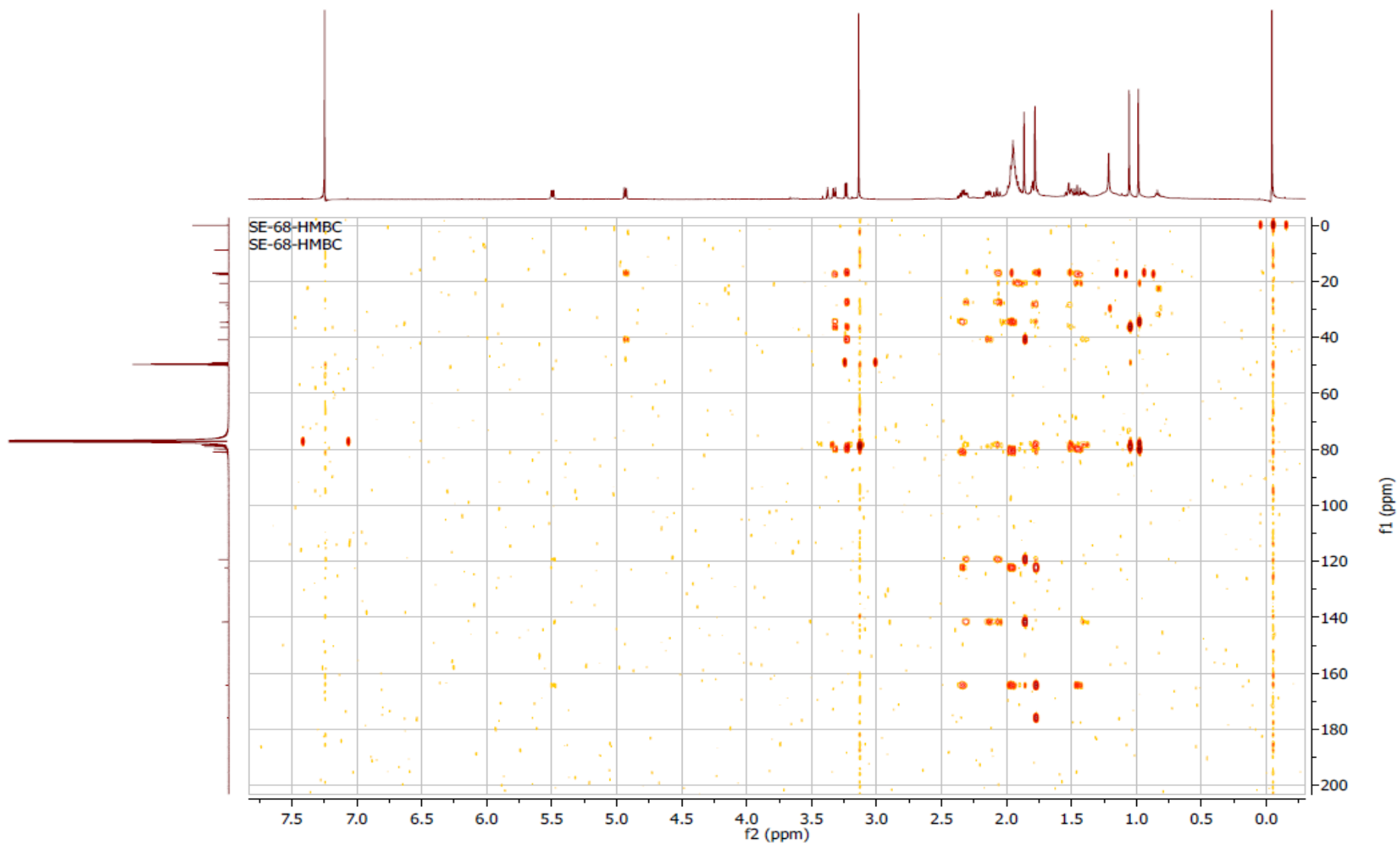




Figure S5. HMBC spectrum of Sarcoehrenbergilid A (1) in CHCl<sub>3</sub>.



Figure

Fig. S6.  $^1\text{H}$ ,  $^1\text{H}$  COSY spectrum of Sarcoehrenbergilid A (1) in  $\text{CDCl}_3$ .

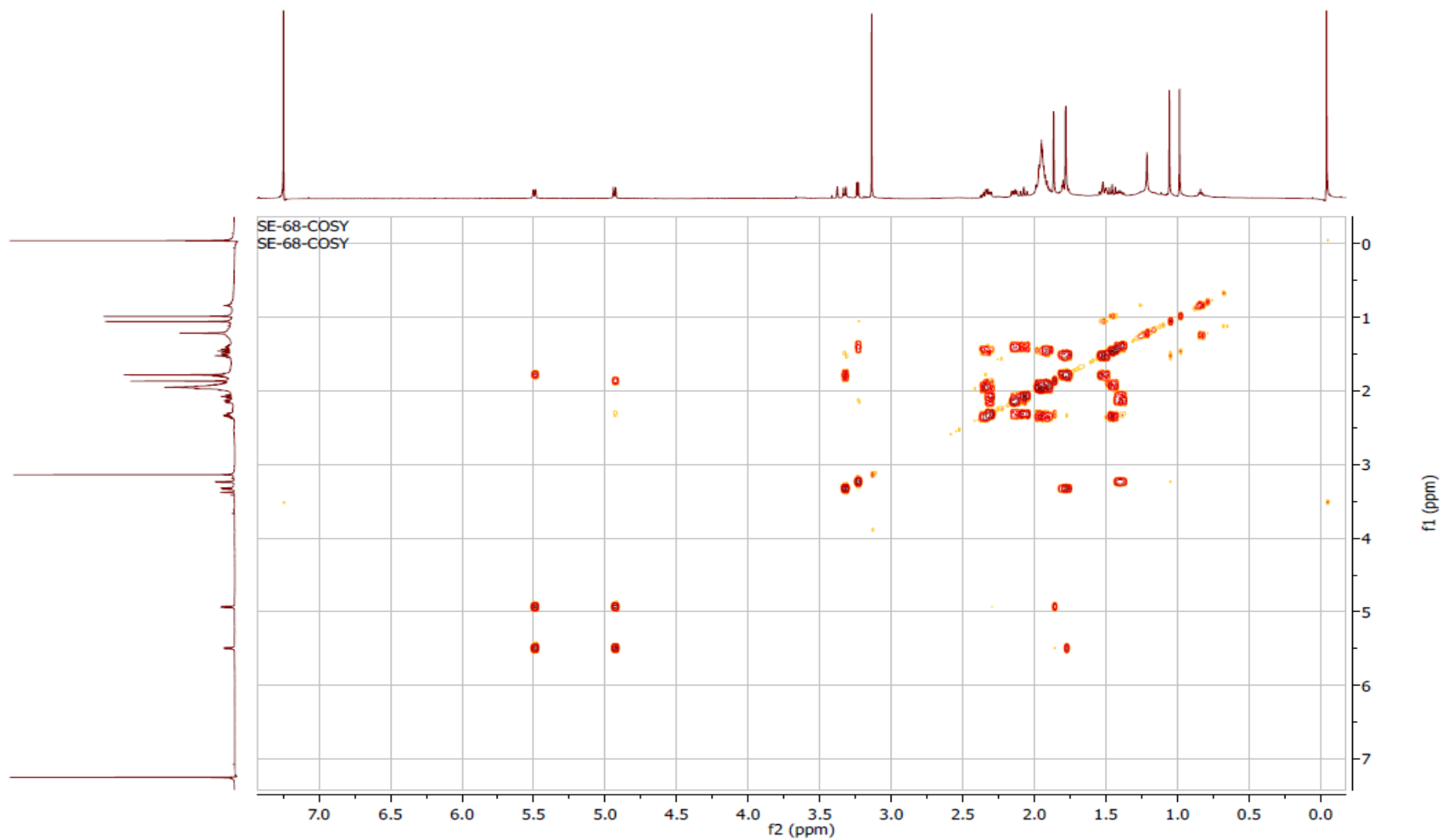


Figure S7. NOESY spectrum of Sarcoehrenbergilid A (1) in CDCl<sub>3</sub>.

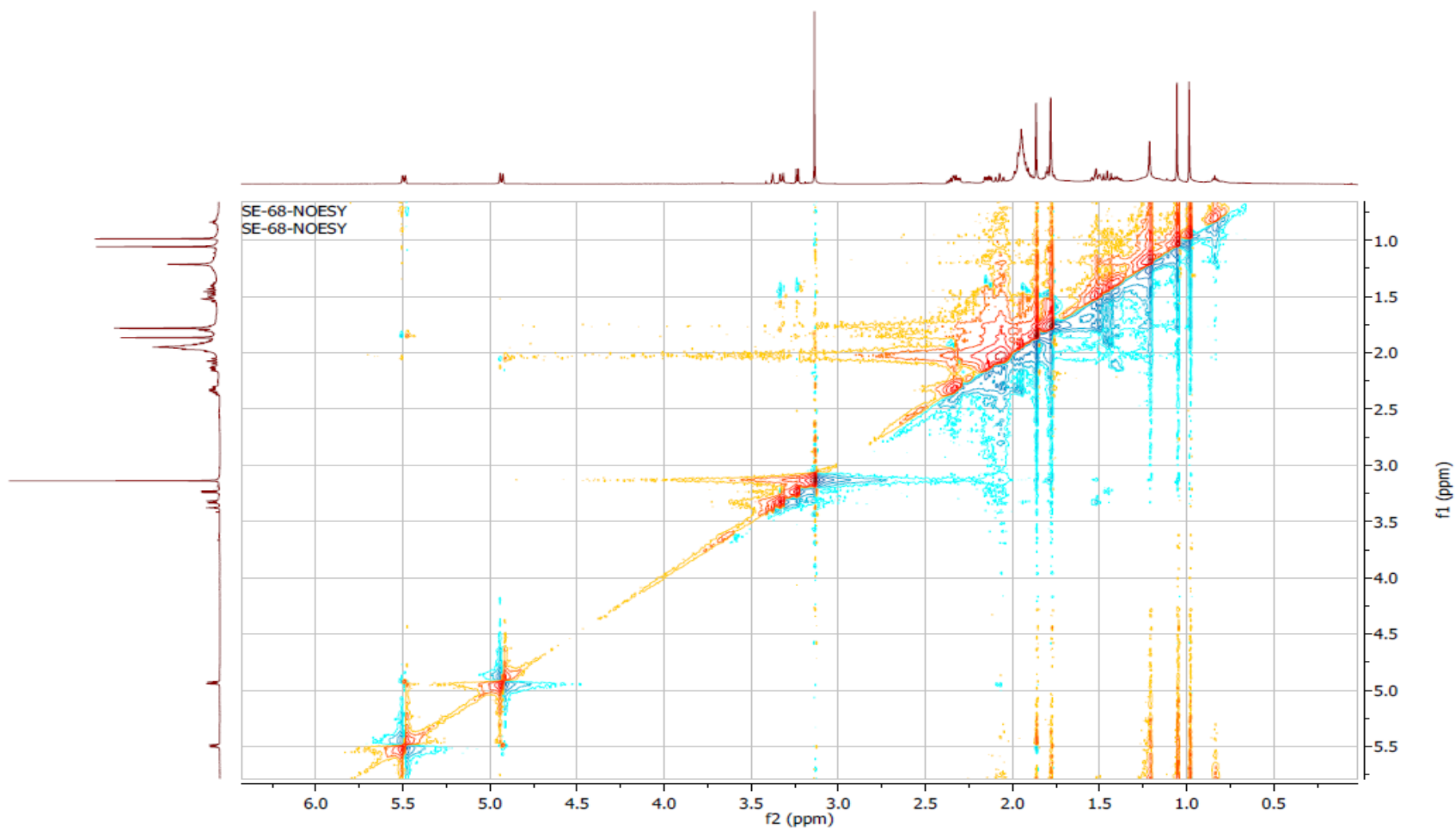


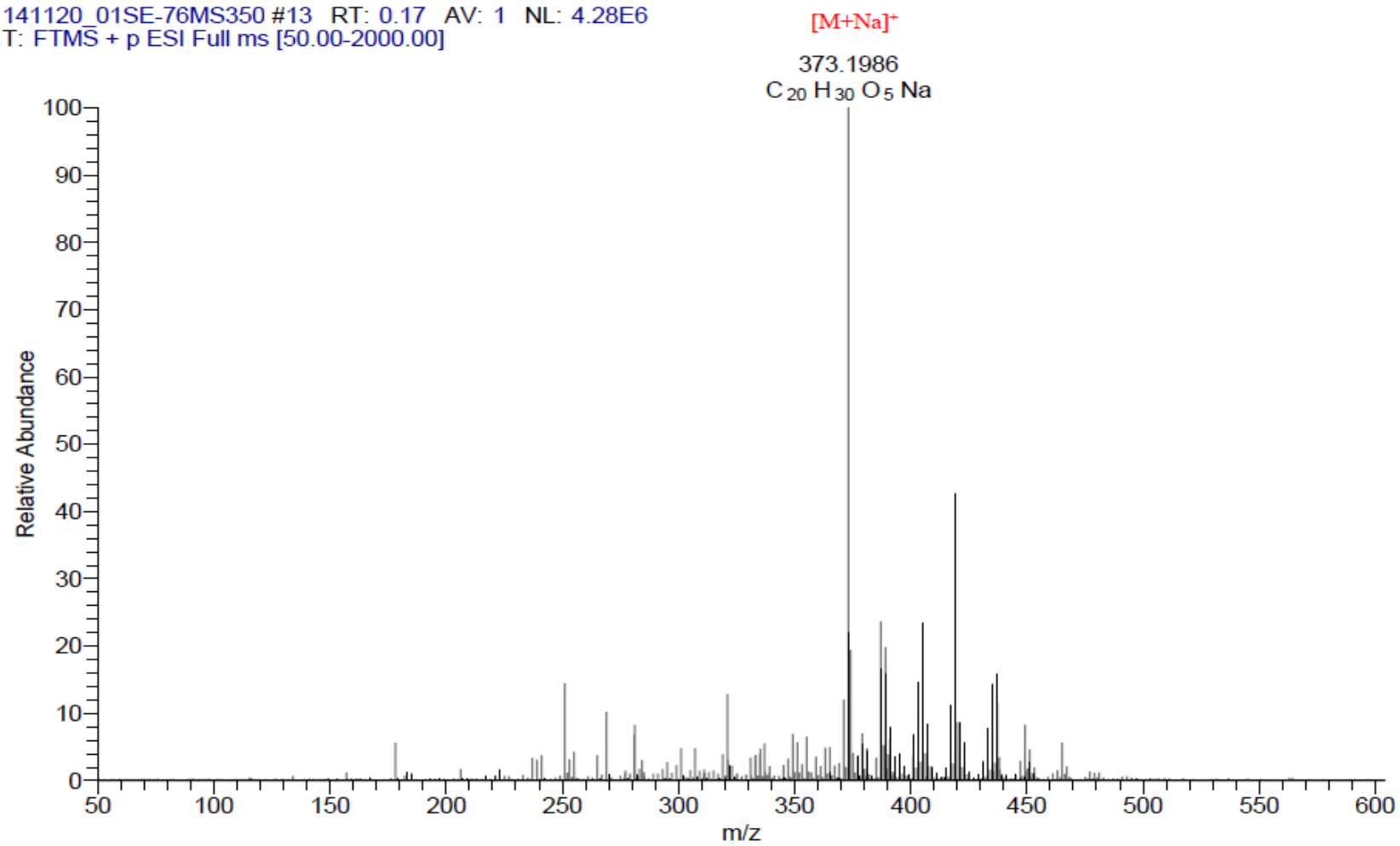
Figure S8. HR-ESI-FTMS spectrum of Sarcoehrenbergilid B (2).

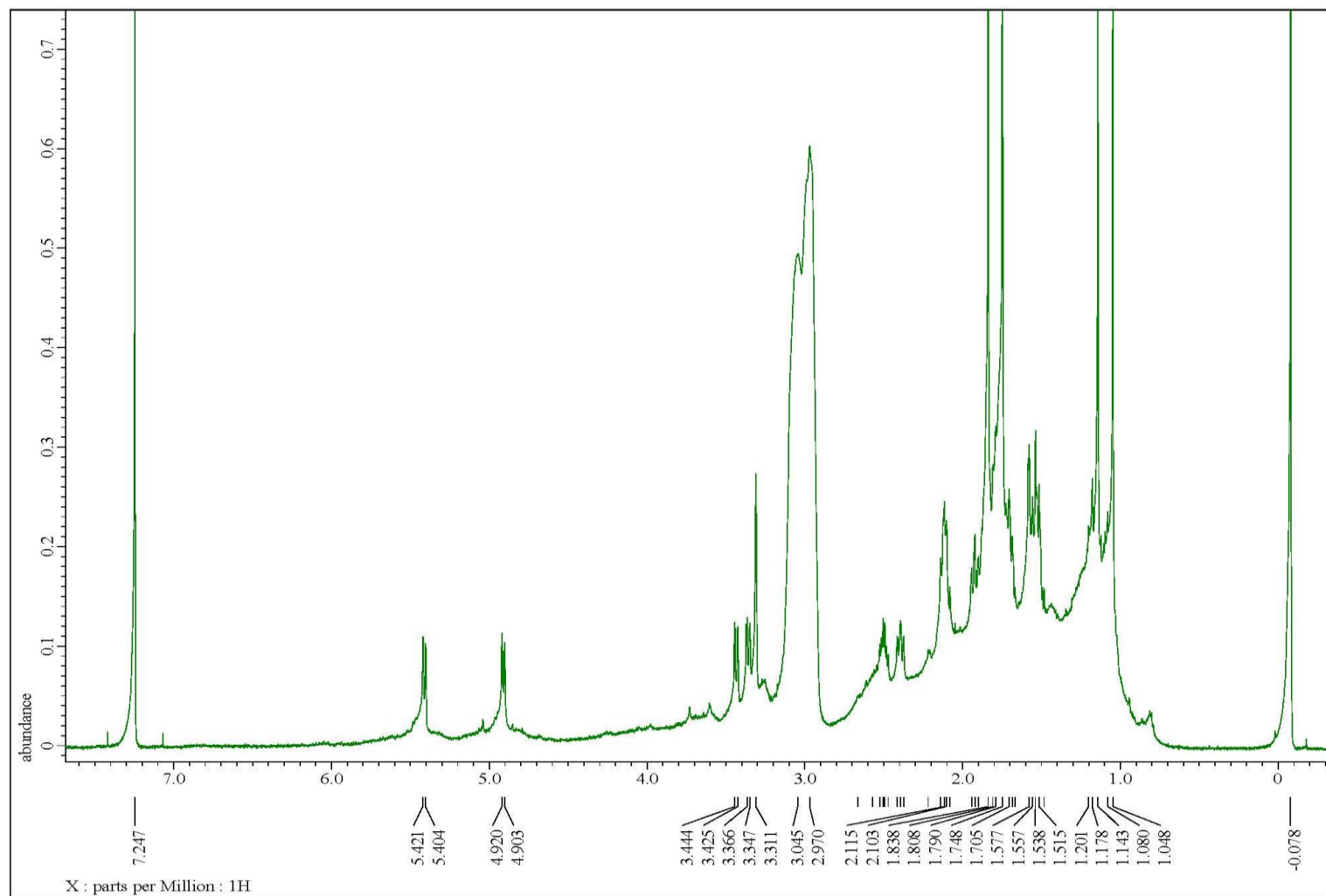
SE-76

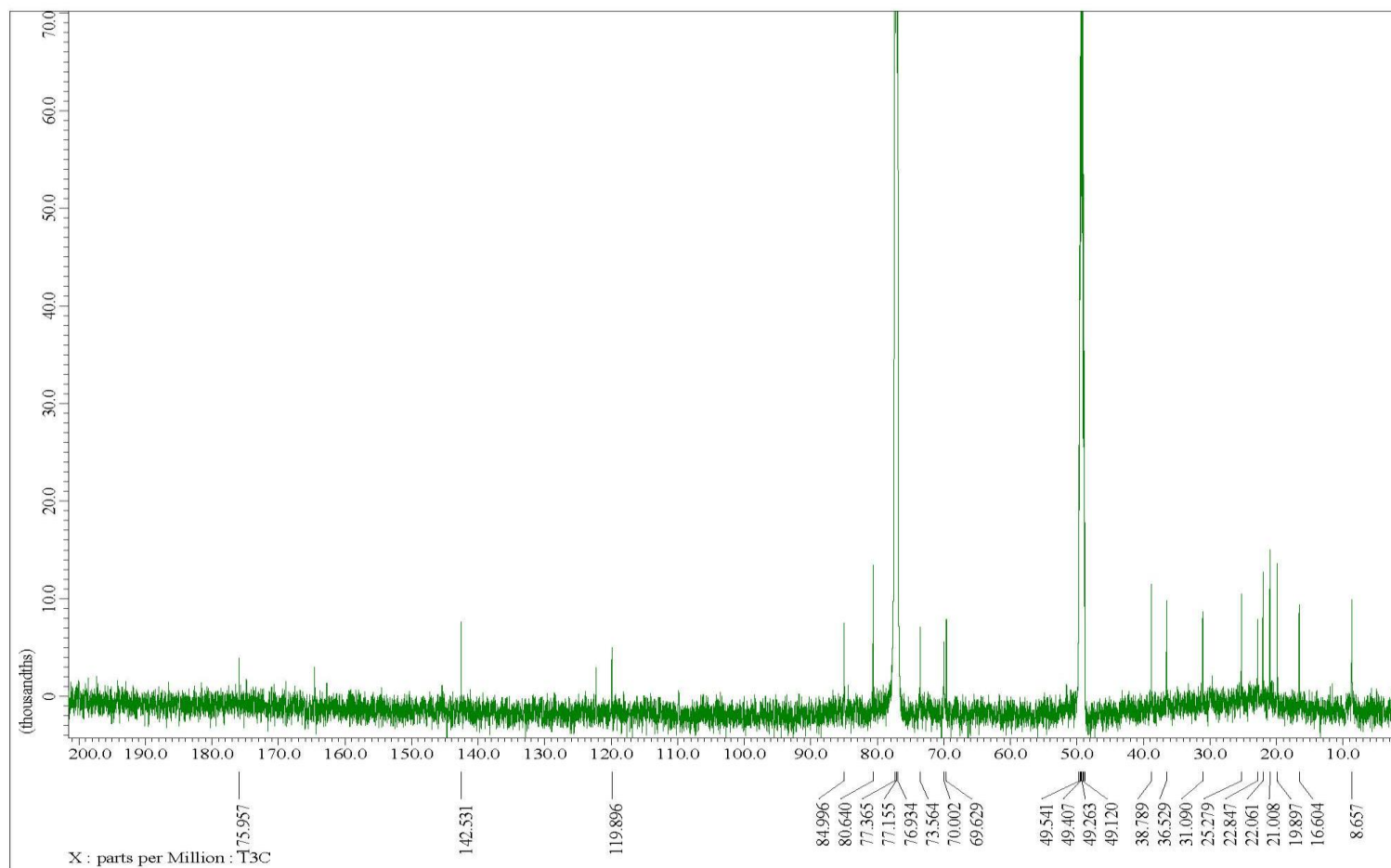
Mw 350

(+)HR-ESI-FTMS

141120\_01SE-76MS350 #13 RT: 0.17 AV: 1 NL: 4.28E6  
T: FTMS + p ESI Full ms [50.00-2000.00]



**Figure S9.**  $^1\text{H}$  NMR spectrum of Sarcoehrenbergilid B (**2**) in  $\text{CDCl}_3$ .

**Figure S10.**  $^{13}\text{C}$  NMR spectrum of Sarcoehrenbergilid B (**2**) in  $\text{CDCl}_3$ .

**Figure S11.**  $^1\text{H}$ - $^1\text{H}$  COSY spectrum of Sarcoehrenbergilid B (**2**) in  $\text{CDCl}_3$ .

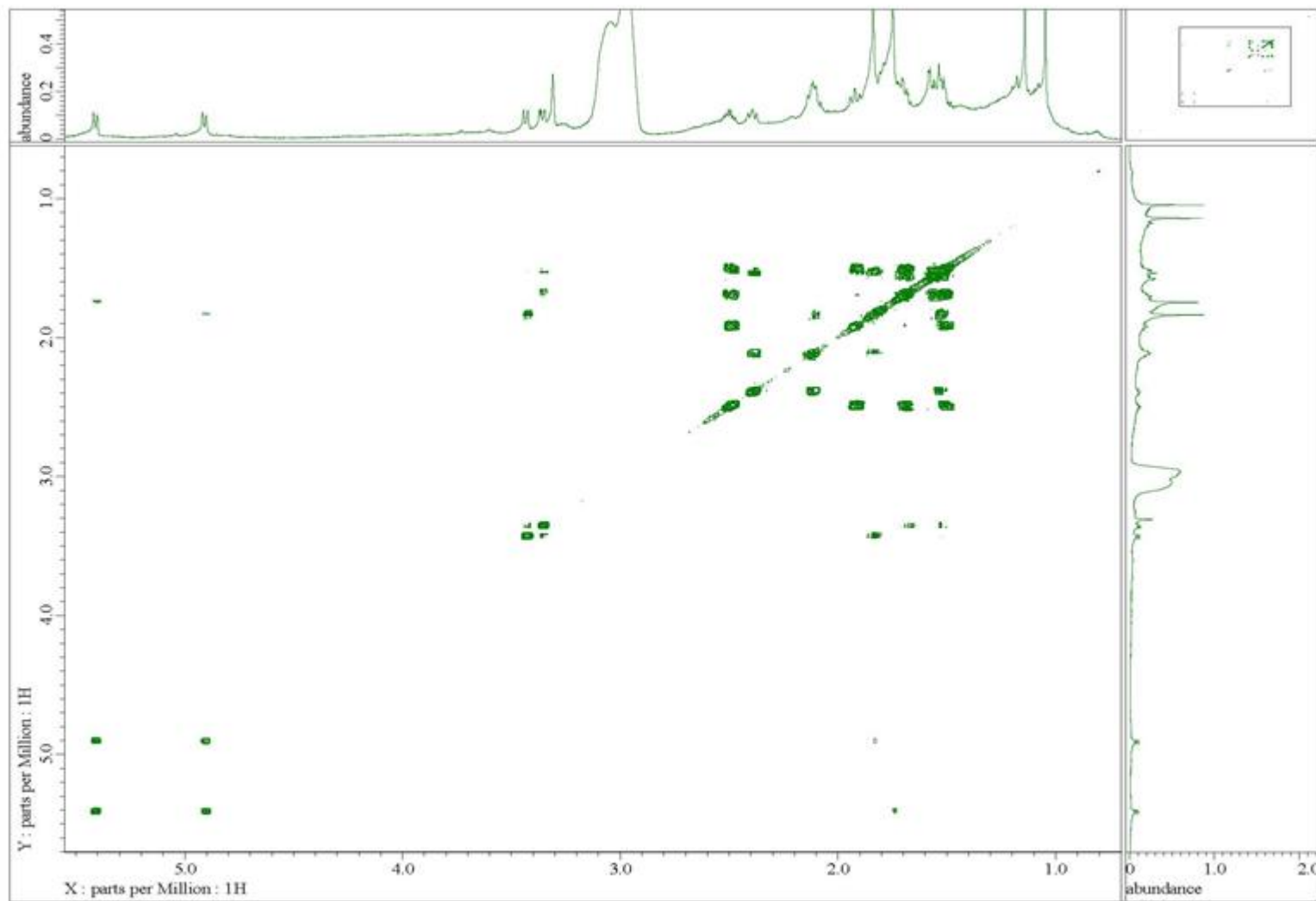


**Figure S12.** HSQC spectrum of Sarcoehrenbergilid B (2) in CDCl<sub>3</sub>.

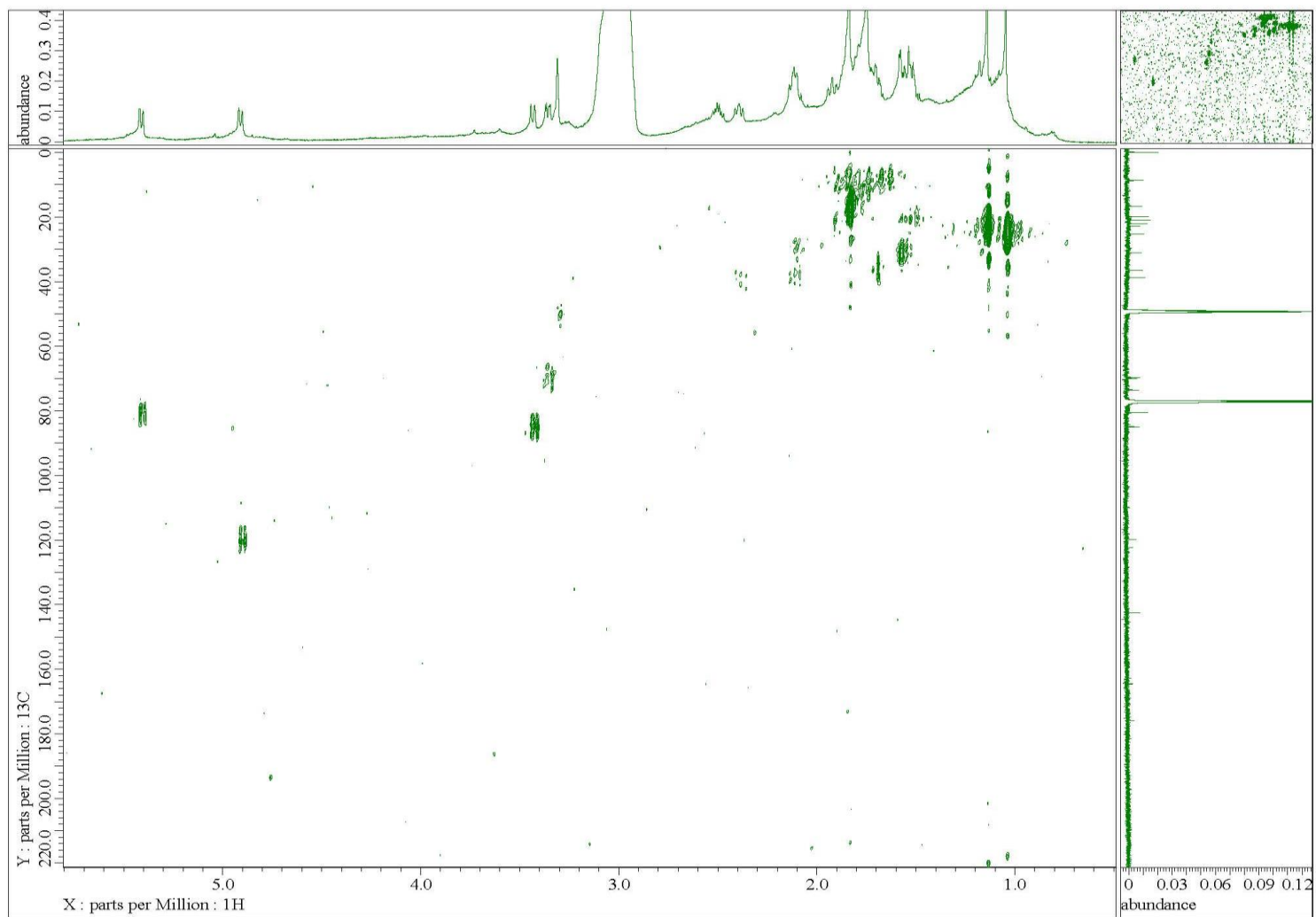
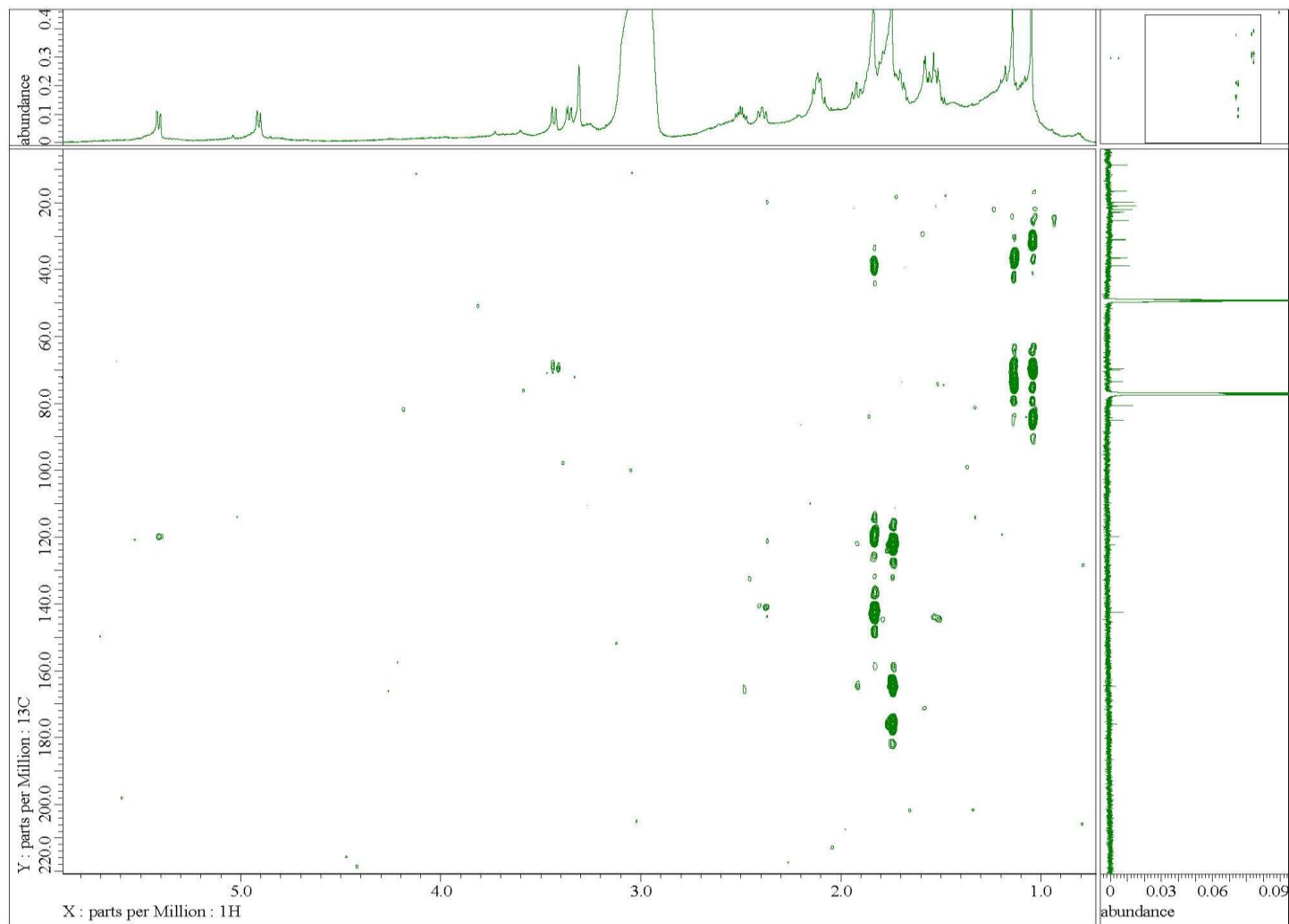
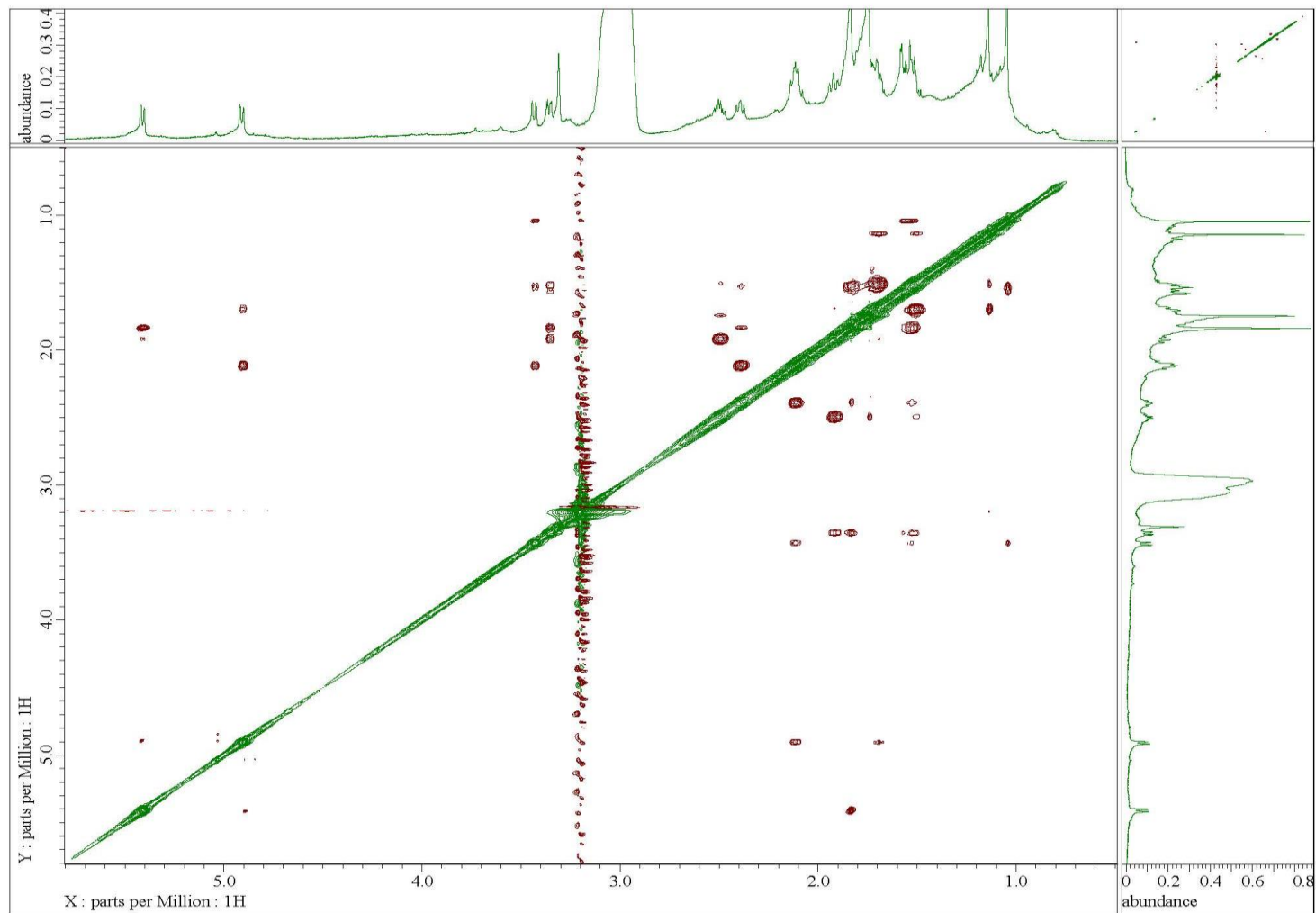




Figure S13. HMBC spectrum of Sarcoehrenbergilid B (2) in CDCl<sub>3</sub>.



**Figure S14.** NOESY spectrum of Sarcoehrenbergilid B (2) in CDCl<sub>3</sub>.



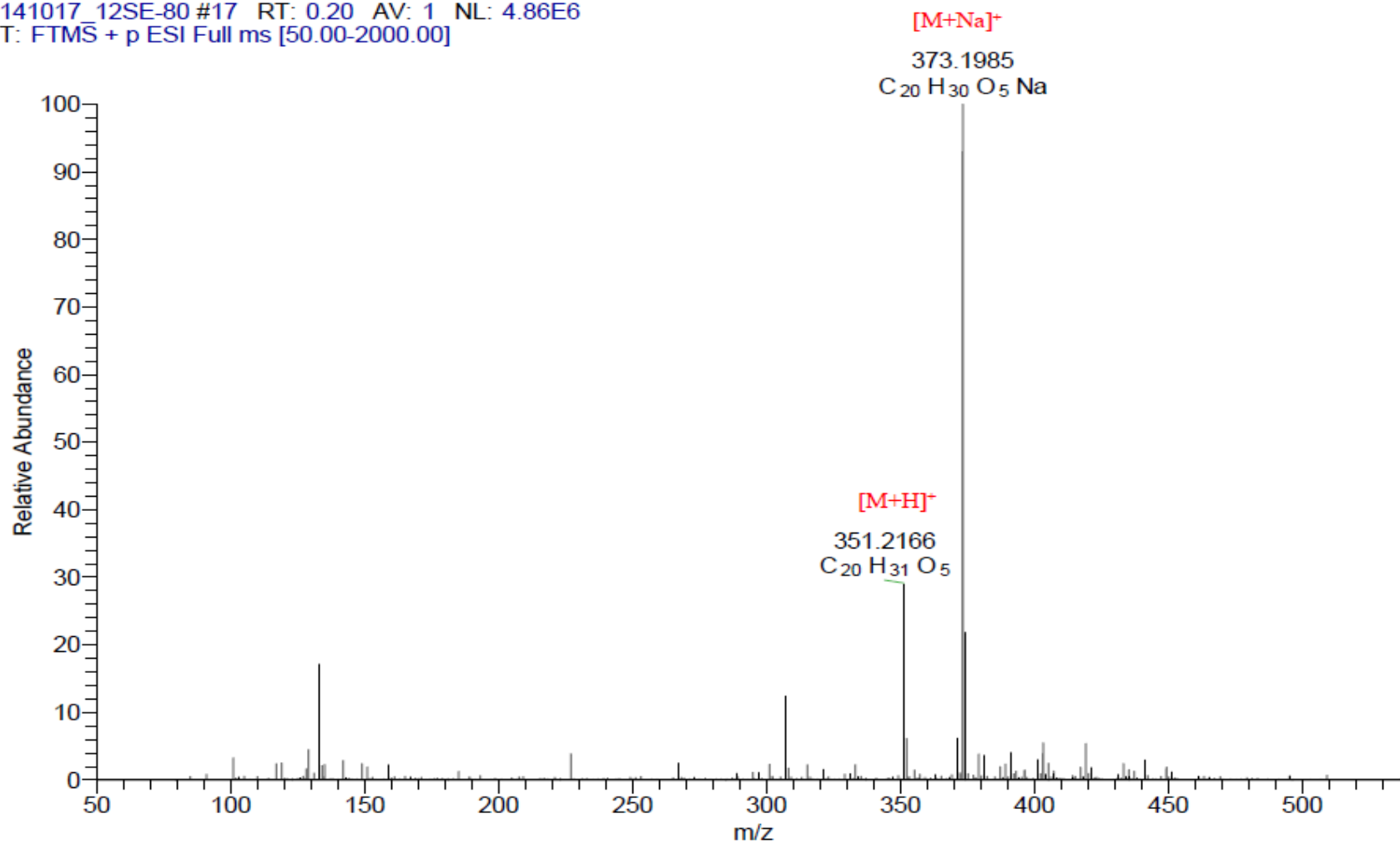
**Figure S15.** HR-ESI-FTMS spectrum of Sarcoehrenbergilid C (3).

SE-80

Mw 350

(+)HR-ESI-FTMS

141017\_12SE-80 #17 RT: 0.20 AV: 1 NL: 4.86E6  
T: FTMS + p ESI Full ms [50.00-2000.00]



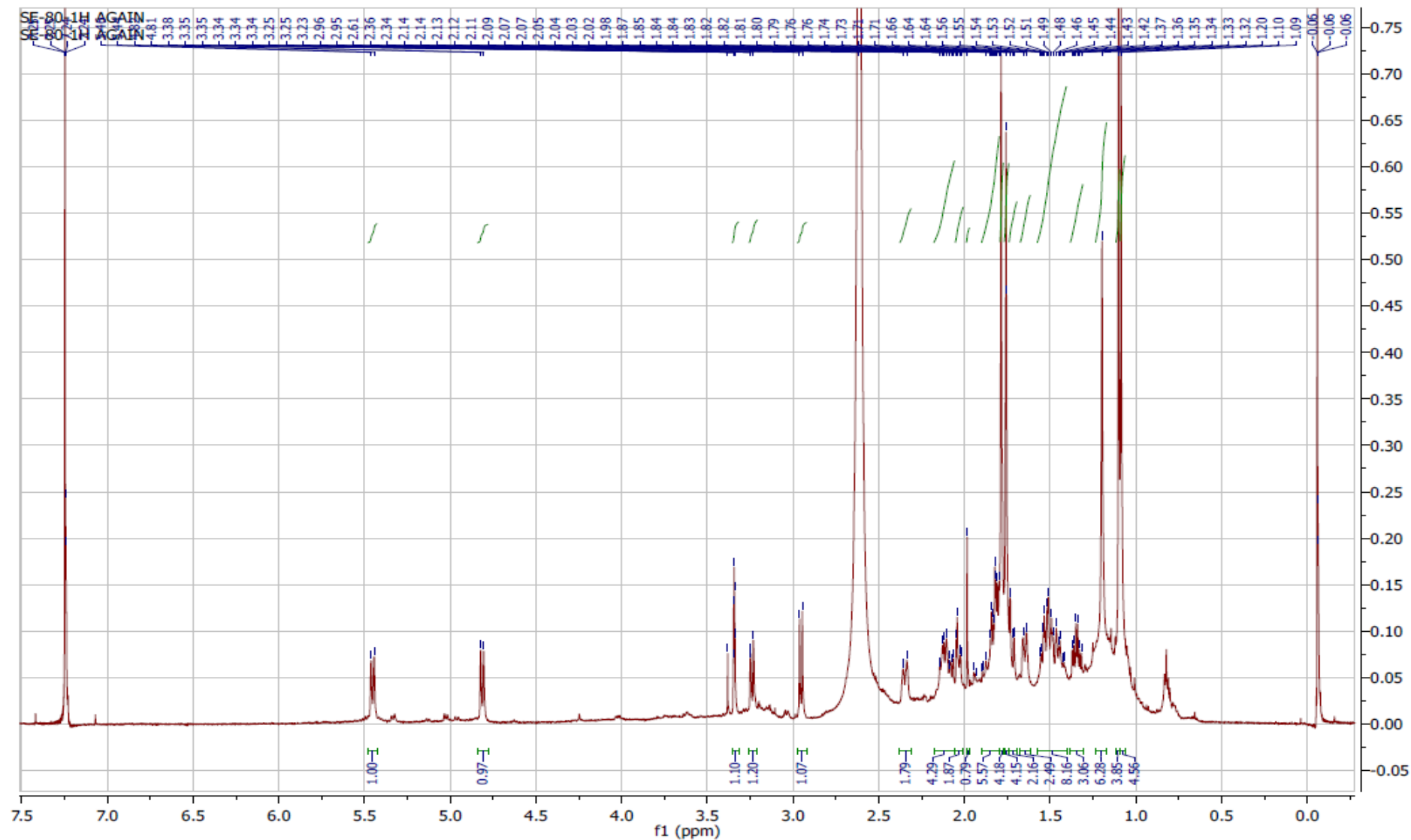
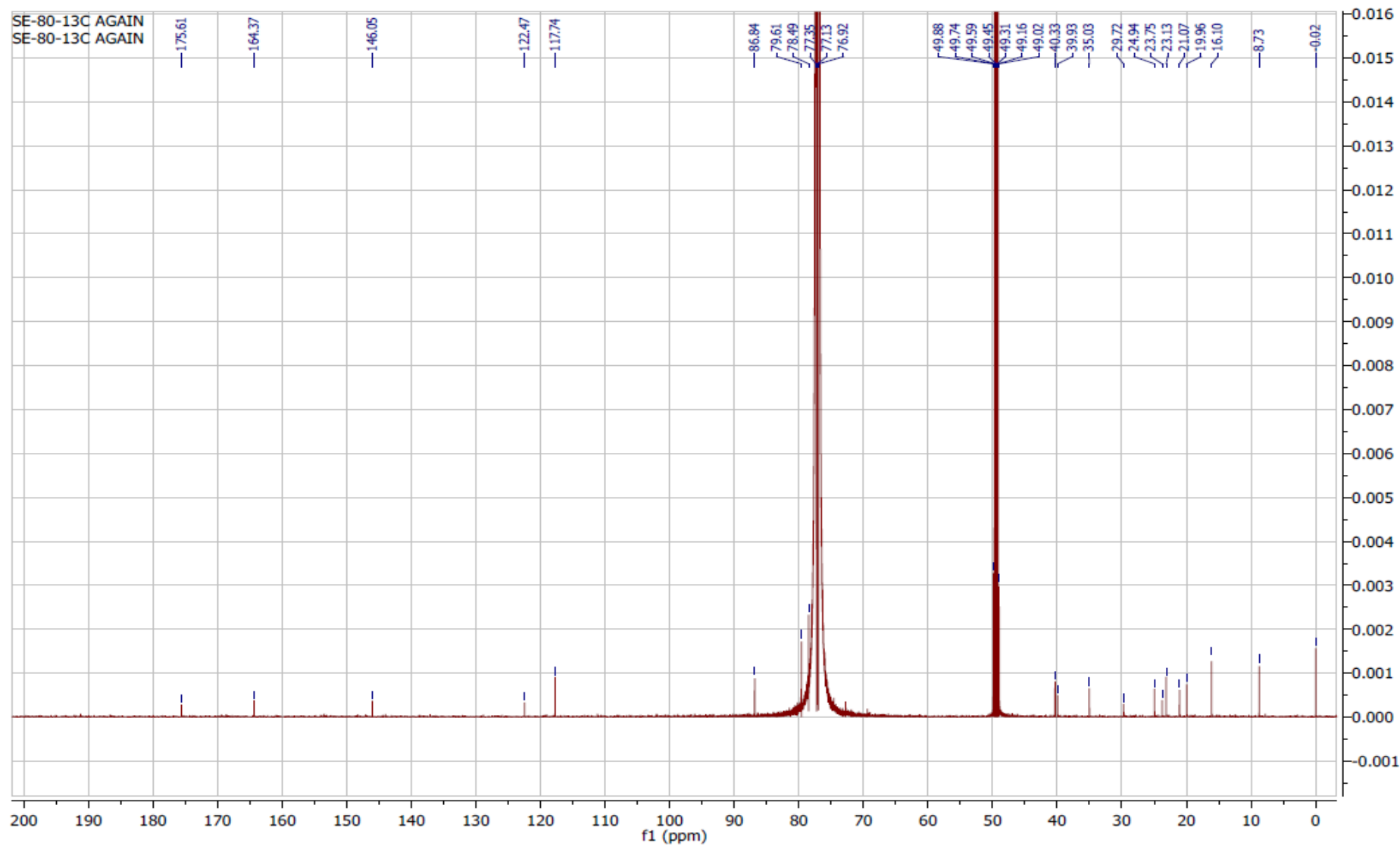
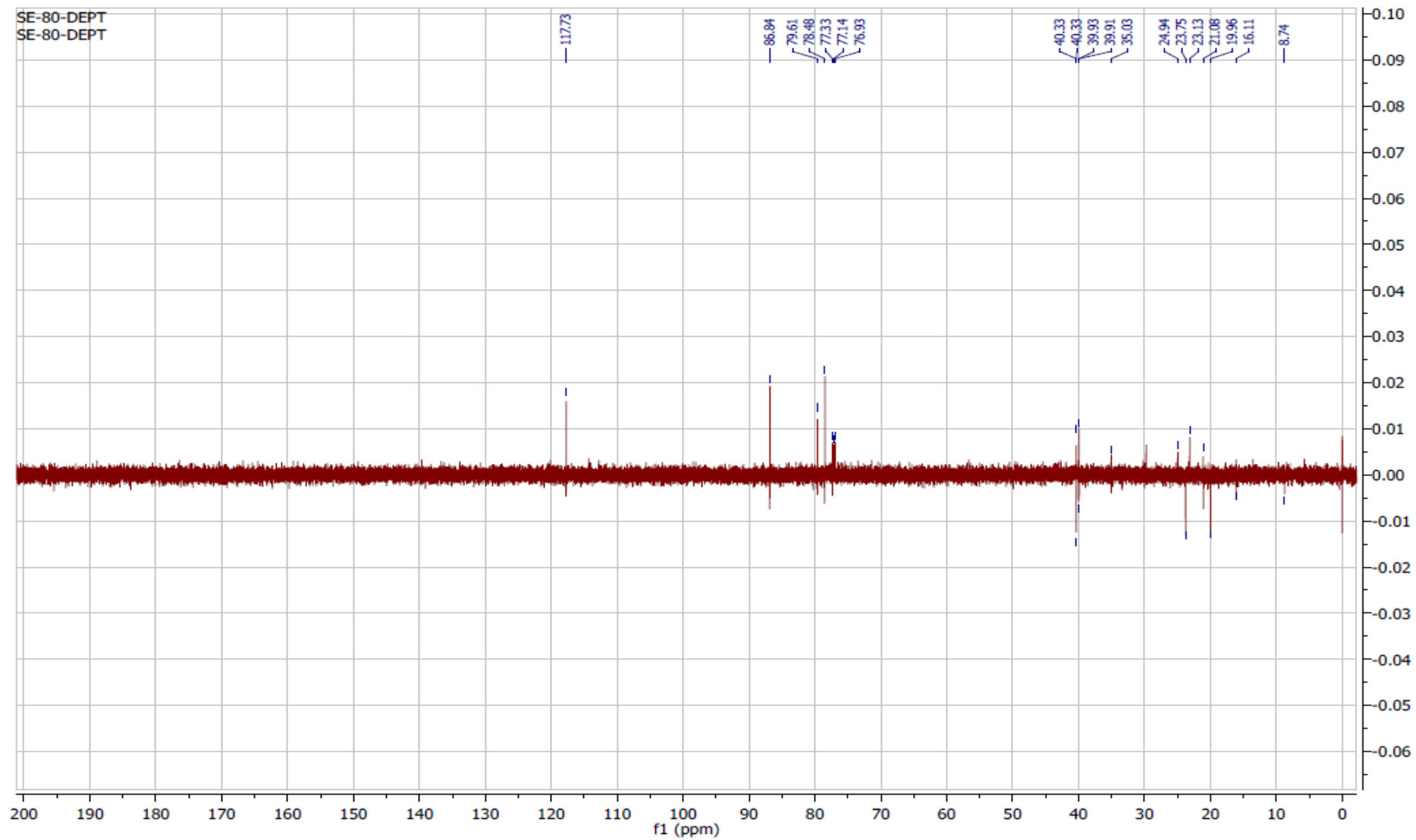
**Figure S16.**  $^1\text{H}$  NMR spectrum of Sarcoehrenbergilid C (**3**) in  $\text{CDCl}_3$ .

Figure S17.  $^{13}\text{C}$  NMR spectrum of Sarcoehrenbergilid C (3) in  $\text{CDCl}_3$ .



**Figure S18.** DEPT spectrum of Sarcoehrenbergilid C (**3**) in CDCl<sub>3</sub>.

**Figure S19.** HSQC spectrum of Sarcoehrenbergilid C (**3**) in CDCl<sub>3</sub>.

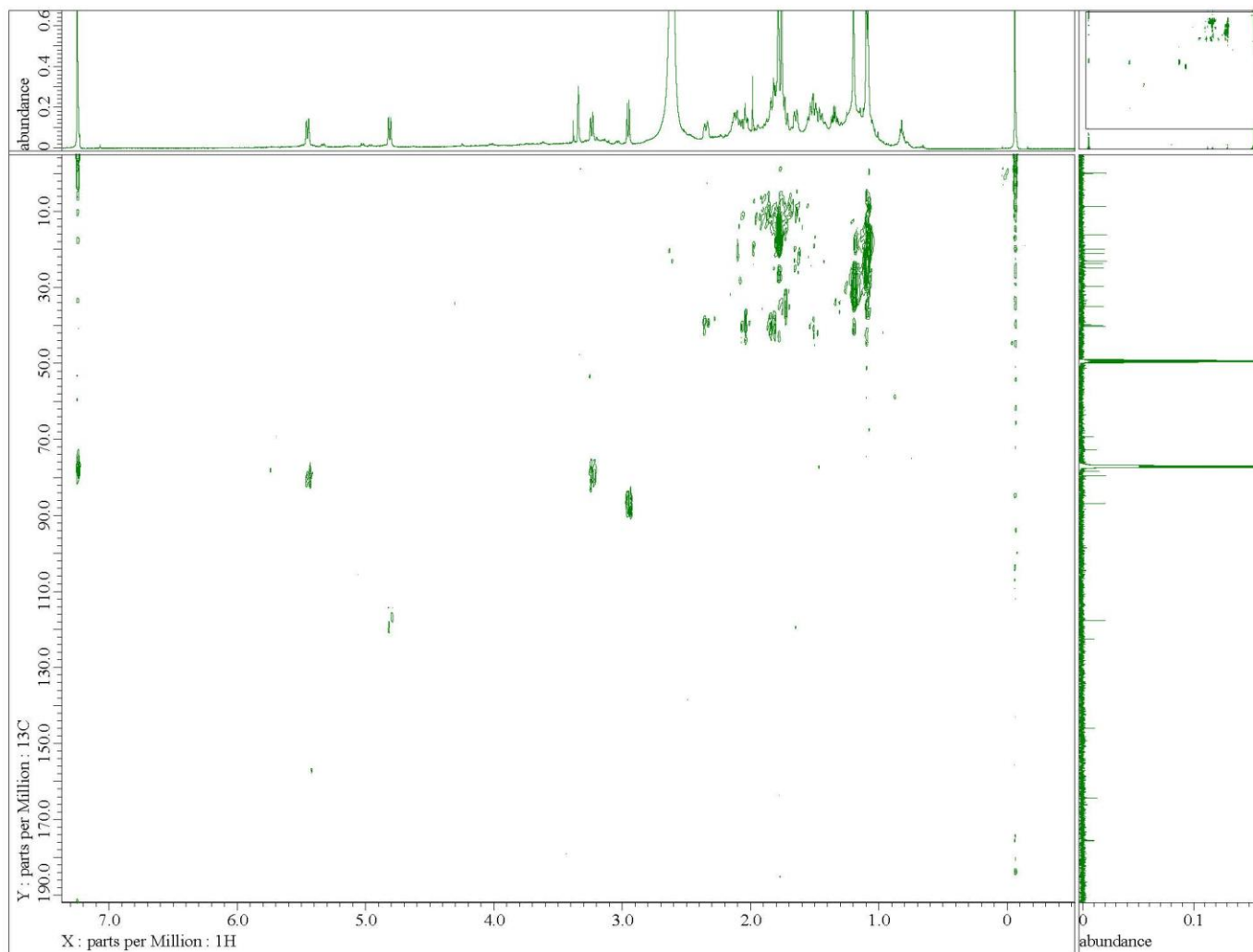
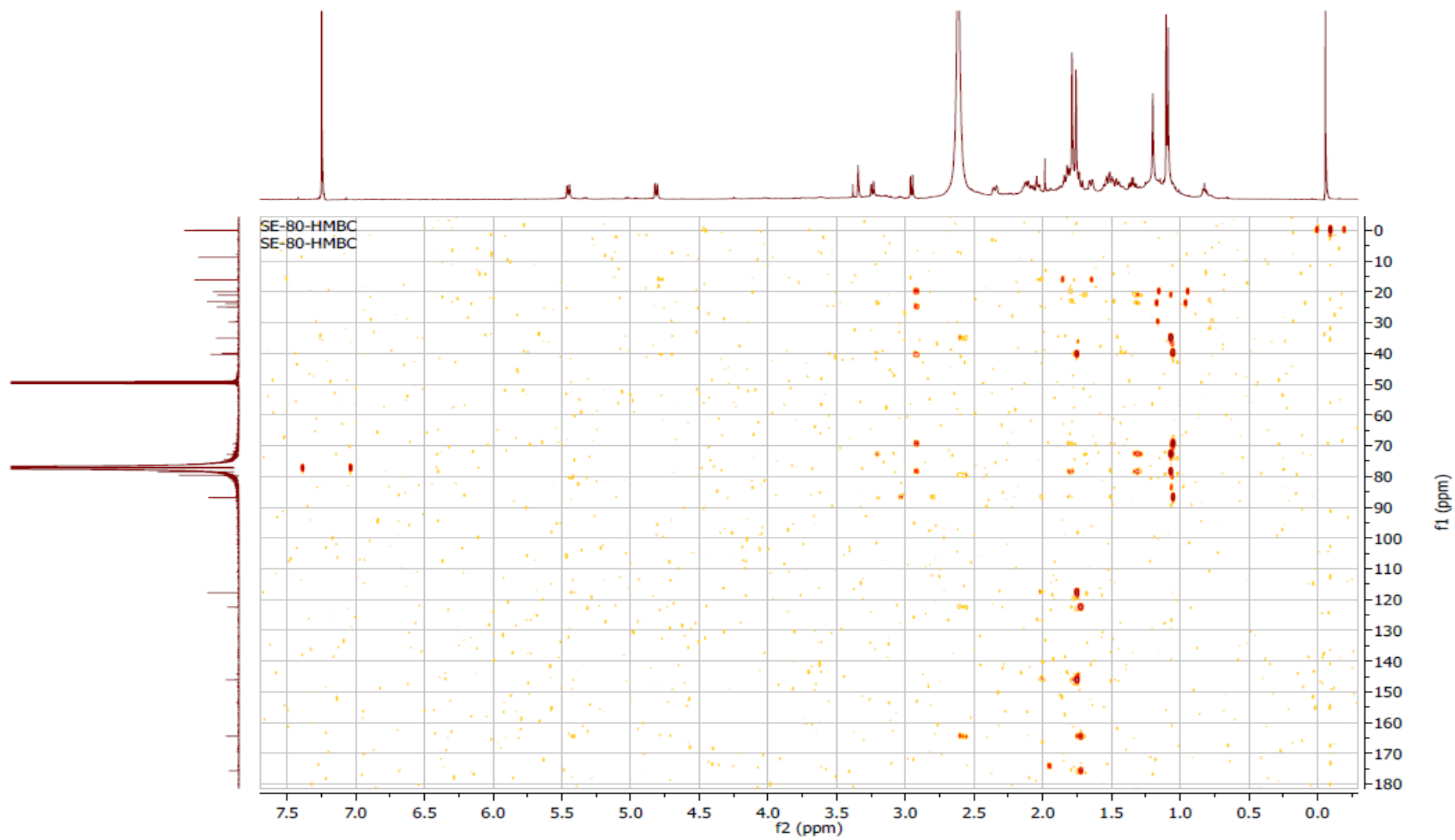
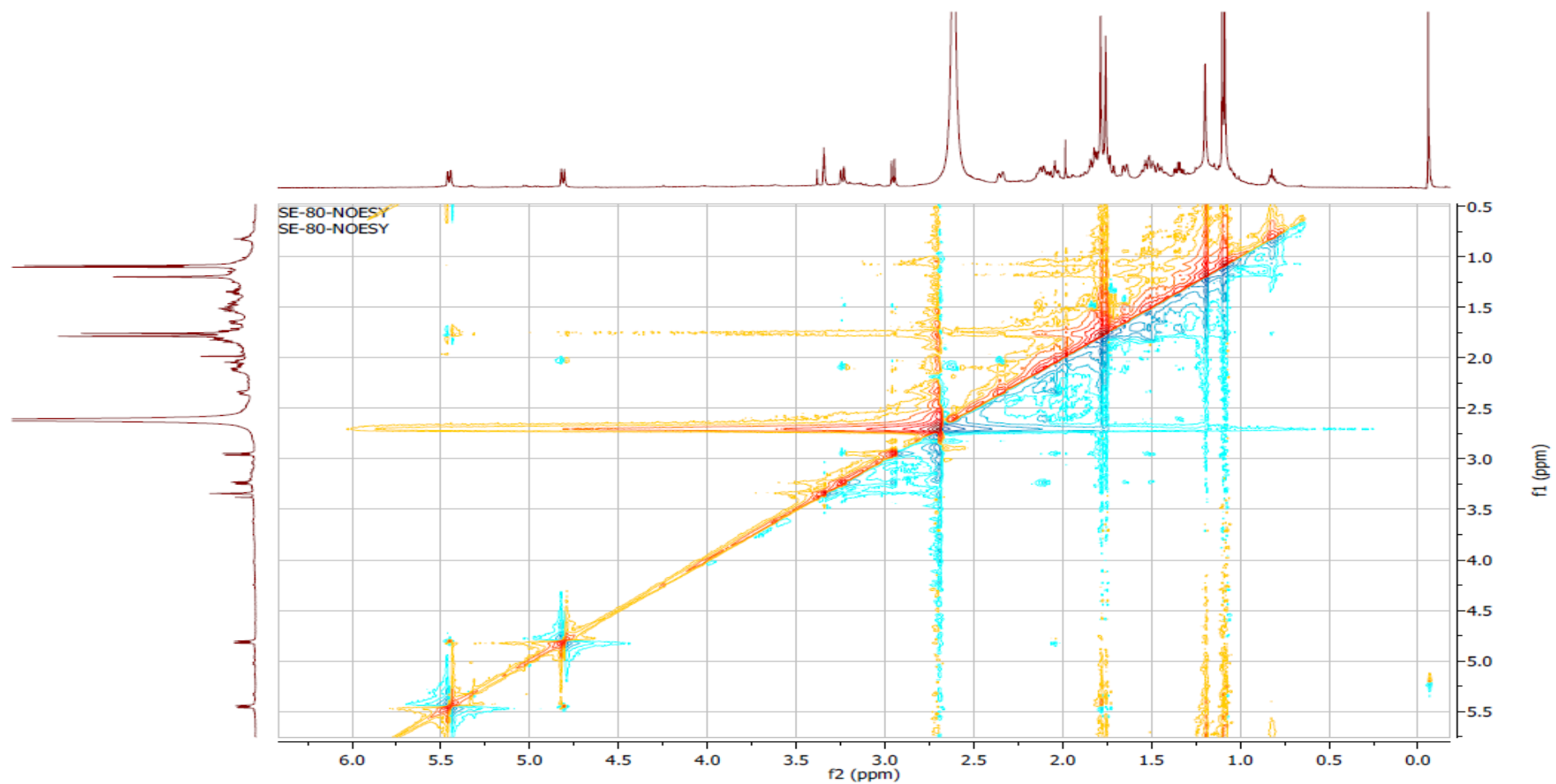


Figure S20. HMBC spectrum of Sarcoehrenbergilid C (3) in CDCl<sub>3</sub>.

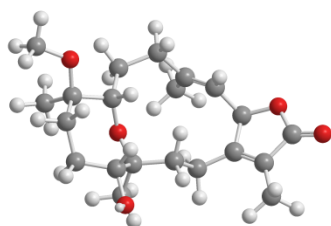




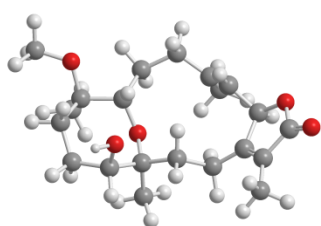
**Figure S21.** NOESY spectrum of Sarcoehrenbergilid C (**3**) in CDCl<sub>3</sub>.



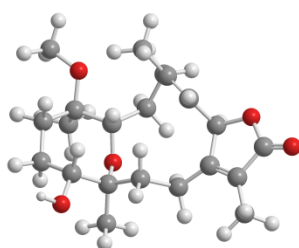
**Figure S22.** Optimized structure and relative free energy of conformers of **1** with Boltzmann population higher than 1%.



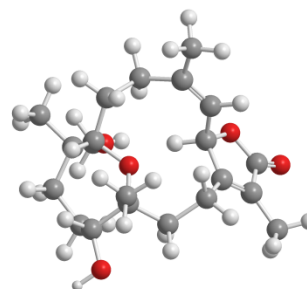
**Compound 1a**



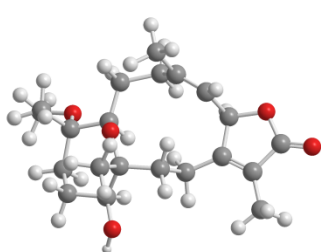
**conformer 1b**  
 $\Delta G=+2.8$  kJ/mol



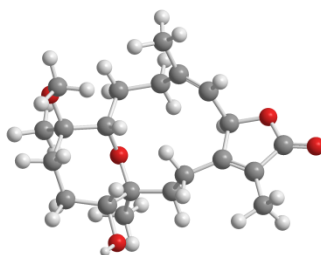
**conformer 1c**  
 $\Delta G=+3.1$  kJ/mol



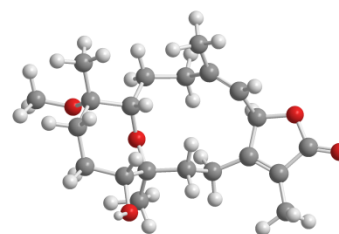
**conformer 1d**  
 $\Delta G=+3.2$  kJ/mol



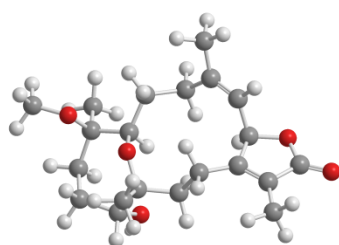
**conformer 1e**  
 $\Delta G=+4.2$  kJ/mol



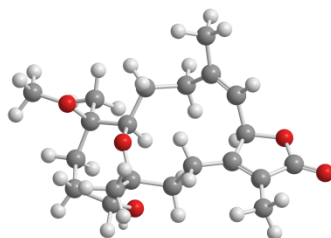
**conformer 1f**  
 $\Delta G=+4.3$  kJ/mol



**conformer 1g**  
 $\Delta G=+5.3$  kJ/mol

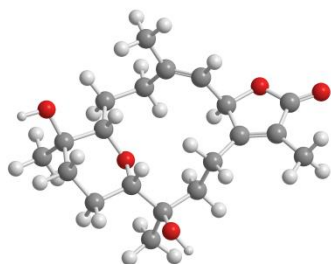


**conformer 1h**  
 $\Delta G=+7.0$  kJ/mol

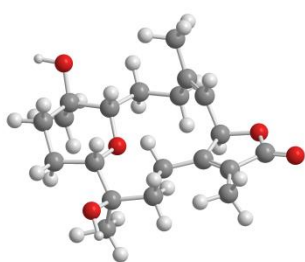


**conformer 1i**  
 $\Delta G=+7.4$  kJ/mol

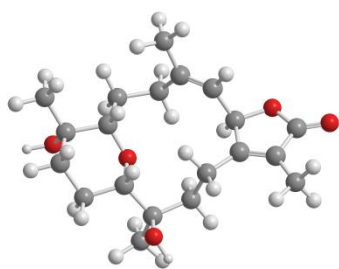
**Figure S23.** Optimized structure and relative free energy of conformers of **2** with Boltzmann population higher than 1%.



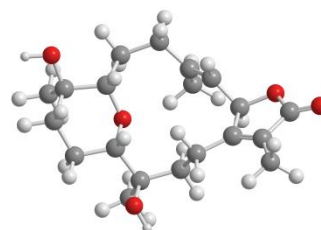
**Compound 2a**



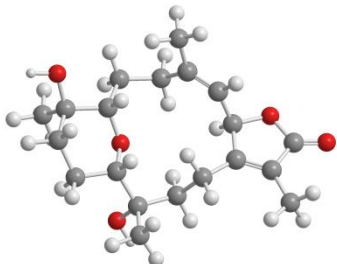
**conformer 2b**  
 $\Delta G=+0.2$  kJ/mol



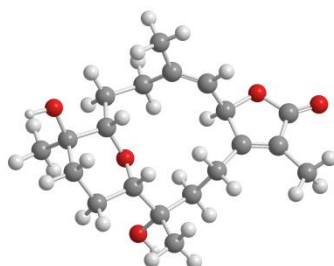
**conformer 2c**  
 $\Delta G=+1.5$  kJ/mol



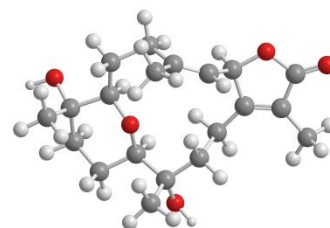
**conformer 2d**  
 $\Delta G=+4.4$  kJ/mol



**conformer 2e**  
 $\Delta G=+6.6$  kJ/mol

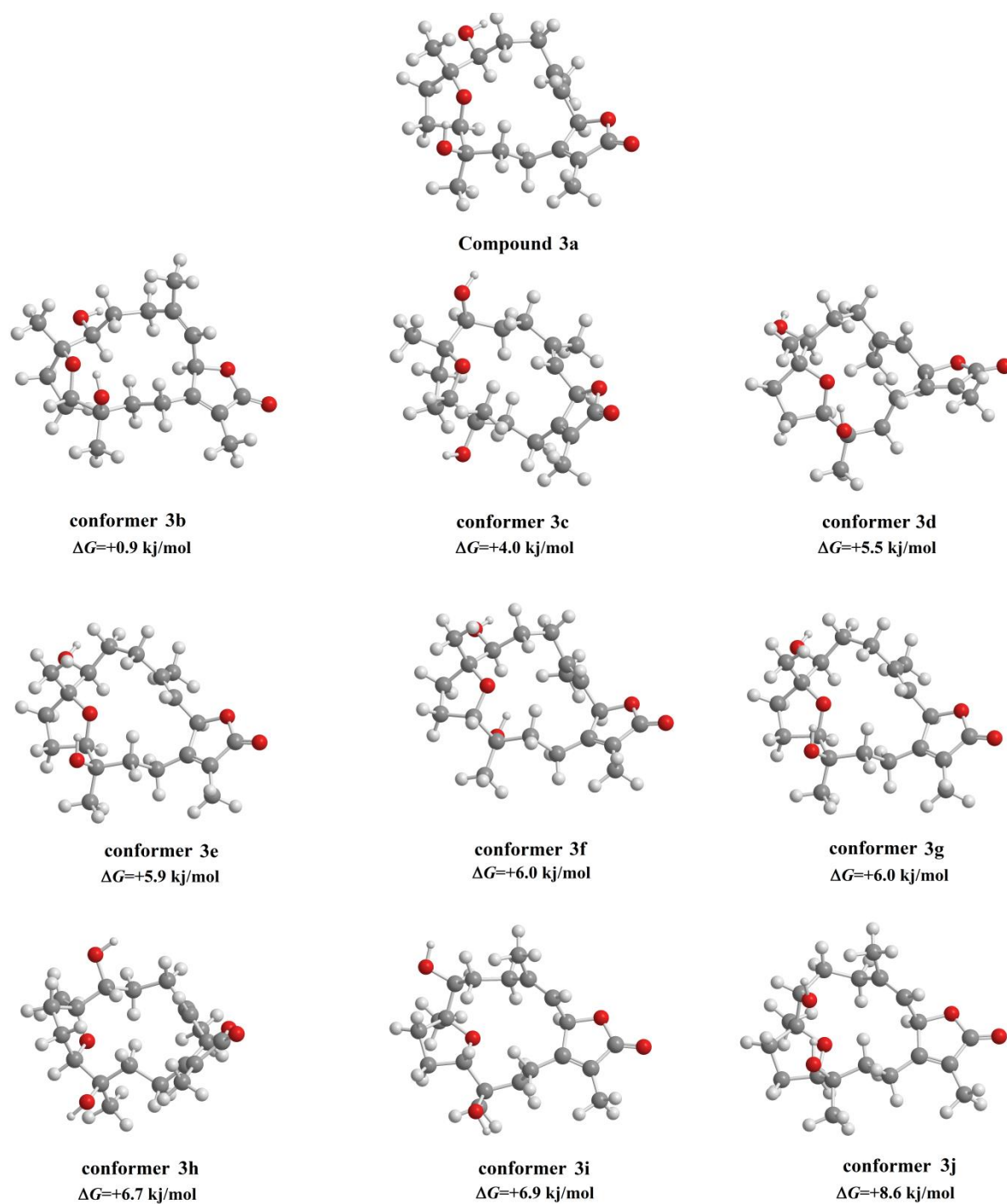


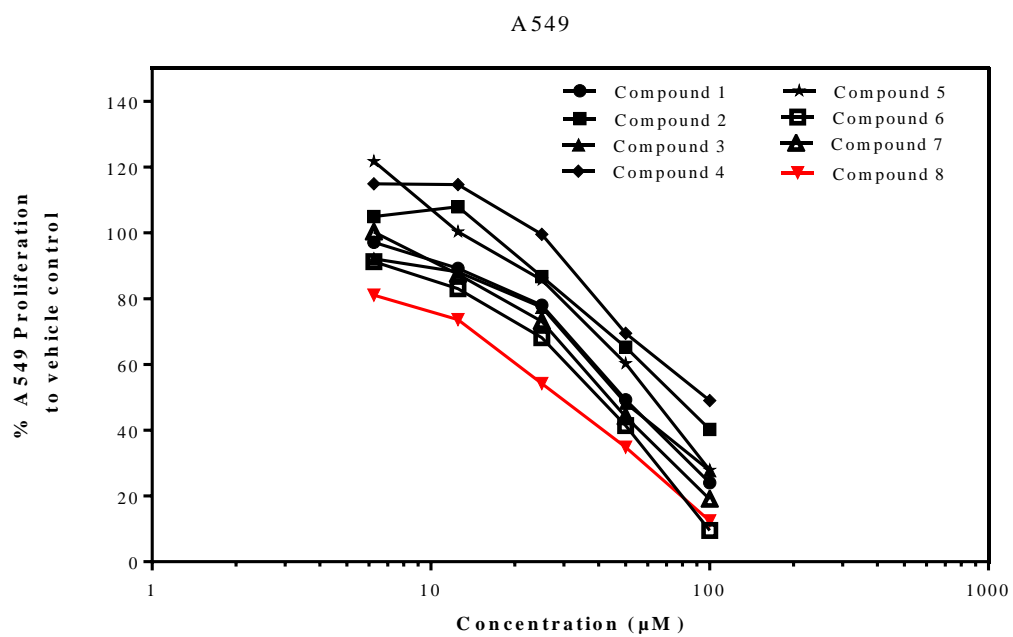
**conformer 2f**  
 $\Delta G=+6.8$  kJ/mol

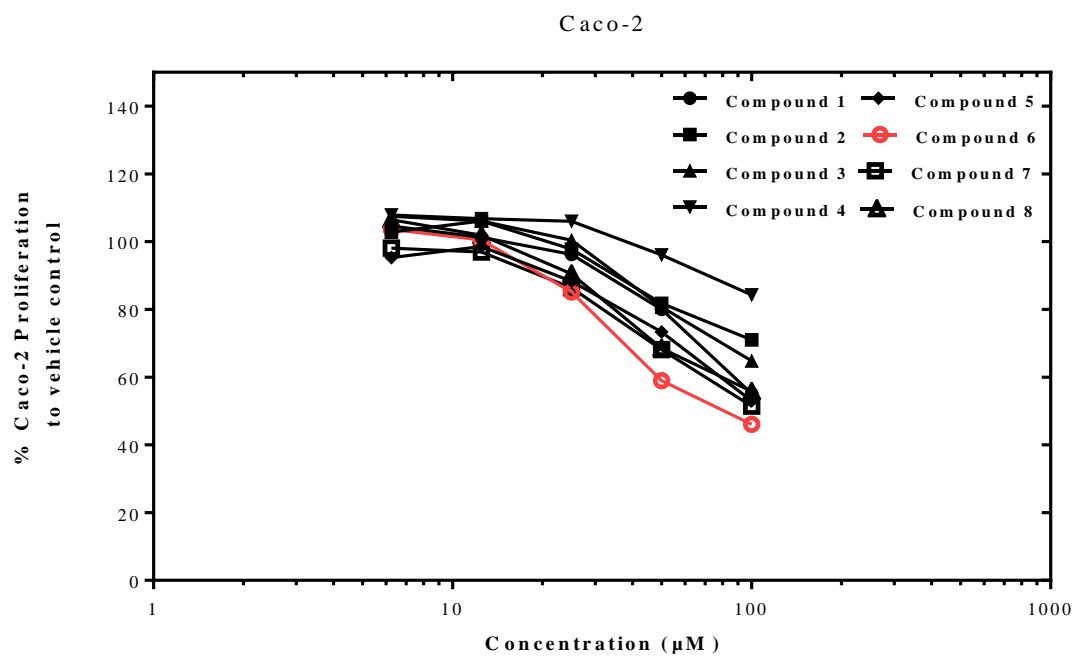


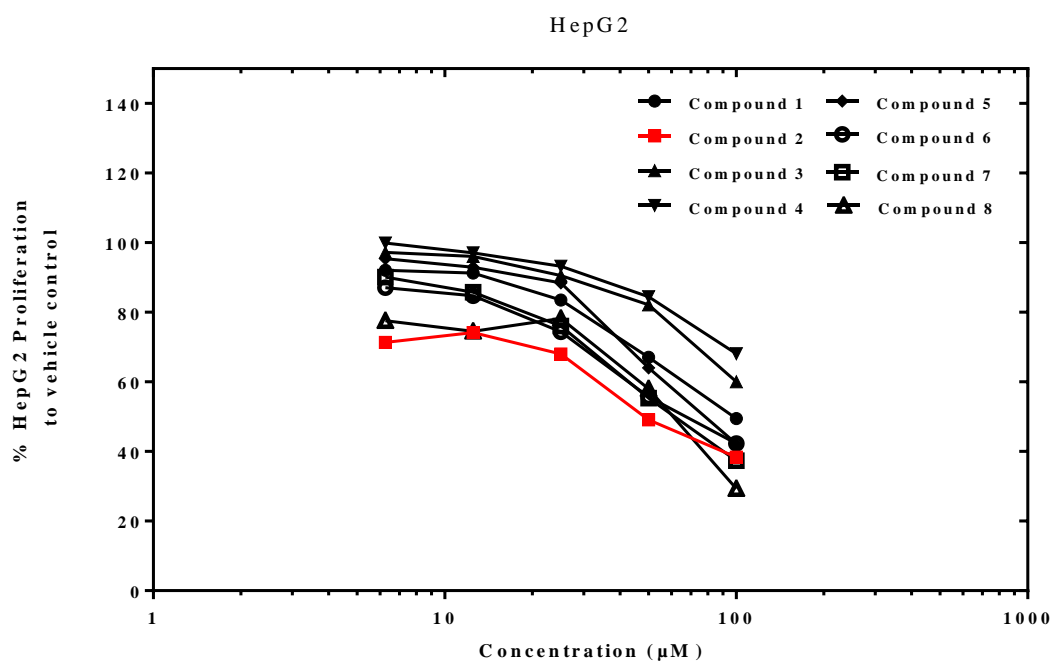
**conformer 2g**  
 $\Delta G=+7.4$  kJ/mol

**Figure S24.** Optimized structure and relative free energy of conformers of **3** with Boltzmann population higher than 1%.

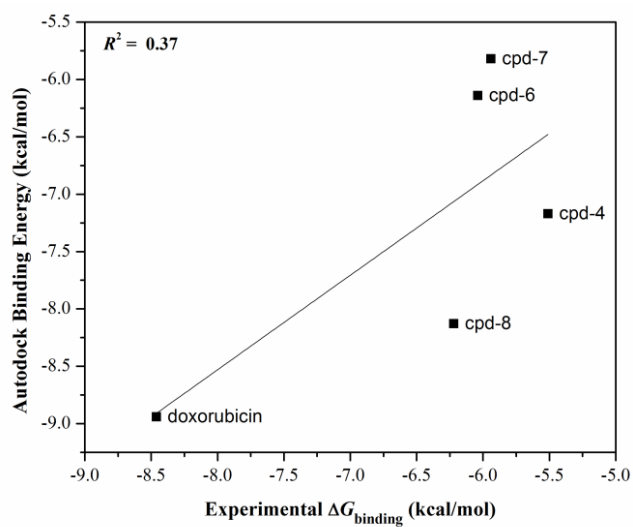


**Figure S25.** Anti-proliferative A549 response curves with 1-8 based on MTT-reduction assay.

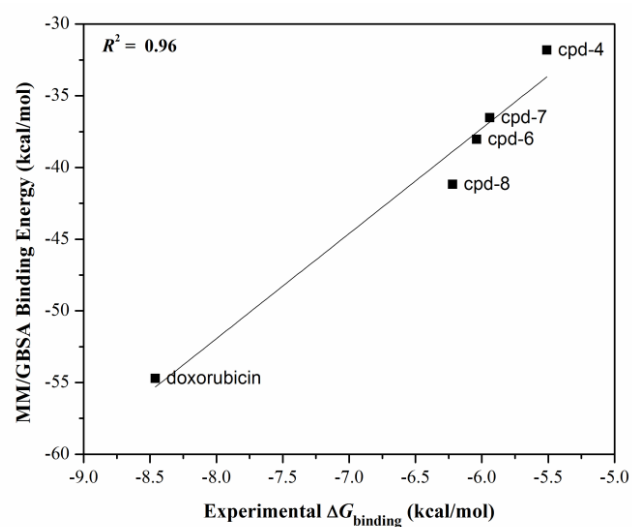
**Figure S26.** Anti-proliferative Caco-2 response curves with 1-8 based on MTT-reduction assay.

**Figure S27.** Anti-proliferative HepG2 response curves with 1-8 based on MTT-reduction assay.

**Figure S28.** Calculated (i) Autodock and (ii) MM/GBSA binding energies of compounds with EGFR kinase domain relative to the experimental binding energies for the tested compounds against A549 cell line.



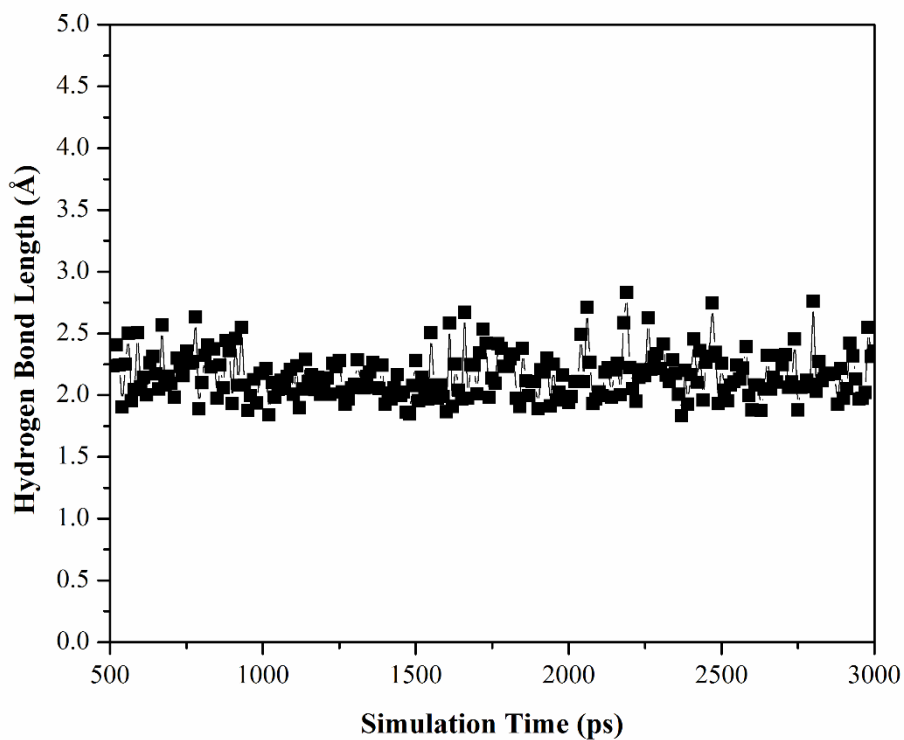
(i)



(ii)



**Figure S29.** Hydrogen bond distance between **8** and carboxylate oxygen atom of Asp<sup>776</sup> inside EGFR active site over a 2.5 ns simulation time.



© 2017 by the authors; licensee MDPI, Basel, Switzerland. This article is an open access article distributed under the terms and conditions of the Creative Commons Attribution license (<http://creativecommons.org/licenses/by/3.0/>).